Efficiency of wollastonite and ammonium polyphosphate combinations on flame retardancy of polystyrene

Yen-Thi-Hai Quach, Laurent Ferry, Rodolphe Sonnier, José-Marie Lopez-Cuesta

Efficiency of wollastonite and ammonium polyphosphate combinations on flame retardancy of polystyrene

Yen-Thi-Hai Quach, Laurent Ferry*, Rodolphe Sonnier and José-Marie Lopez Cuesta

The thermal and fire properties of polystyrene (PS) flame retarded by a system composed of ammonium polyphosphate (APP) and wollastonite (W) were investigated by thermogravimetric analysis, pyrolysis-combustion flow calorimeter, pyrolysis gas chromatography mass spectrometry, cone calorimetry and epiradiator. The combustion residues were observed by scanning electron microscopy/energy dispersive X-ray spectroscopy and analyzed by X-ray diffraction. The combination of both additives enables increasing the thermal stability of PS while increasing simultaneously the high temperature residue. The peak of HRR was also significantly reduced while time to ignition varied depending on the composition. It was shown that the degradation pathway of PS was affected by the presence of the additives implying a reduction of the effective heat of combustion. In the condensed phase, APP decomposition promotes char formation and favors the reactivity between phosphorus and silicate. A layer composed of char, W and a mixture of calcium and silicon phosphate is formed at the sample surface during combustion. This layer is cohesive enough to limit the release of combustible gases to the gas phase. Moreover, the thermally stable protective layer reaches high temperature enabling the re-irradiation of a part of the incident heat flux. The flame retardancy of PS is thus enhanced.

Keywords: polystyrene; wollastonite; ammonium polyphosphate; flame retardancy

INTRODUCTION

The potential of using inorganic minerals as fillers in polymeric composites for improving their thermal stability and their fire retardancy has been demonstrated by many papers in the literature.[1–9] Such fillers become appreciated in commercial applications. Mechanisms of fire retardancy induced by mineral particles have been detailed by various authors,[10–13] highlighting physical effects such as formation of mineral barriers able to limit volatile and oxygen transfer, and chemical effects like the formation of carbonaceous residues due to catalytic processes.[14]

The research about the thermal stability and fire behavior of composites based on polystyrene (PS) is exploited commodiously.[2,3,15–17] Some of our previous works in the laboratory have investigated PS composites prepared via melt blending. Various fillers such as alumina, modified alumina, silica and modified silica have been incorporated into PS.[14,18–20] Beside the treatment of the filler surface, the combination of mineral particles with ammonium polyphosphate (APP)[14] which can act as a flame retardant producing an intumescent structure (expanded char layer) was also investigated. Synergistic effects on HRR and thermal stability between the aluminas, silicas and APP were noticed. With the aim to find new synergistic effect between APP and other filler, wollastonite (W) was chosen because of its thermal stability. W, also known as calcium metasilicate, is a naturally occurring mineral. It has been used usually in polymer composites as mechanical reinforcement[21–24] and thermal stabilizer.[25] Some authors showed also the efficiency of W as flame retardants in the silicone-based materials[6,26,27] and in PA-66.[28,29] In this paper, the combination of W with APP was investigated as flame-retardant system in PS. Different ratios of W and APP have been incorporated in the PS. Thermal and flammability properties have been studied, evaluated and discussed.

EXPERIMENTAL

Materials

Pellets of PS (Total Petrochemicals, crystal PS 1960N) were milled into powder form using a Pallman crushing machine before blending with additives. Commercial W $CaSiO_3$ (NYAD 5000) was supplied by Nyco minerals. W belongs to the inosilicate group and exhibits a triclinic crystal structure. Its crystal habit is commonly fibrous aggregates as can be seen in Fig. 1. Its median particle size is about 2.2 μm, and its BET specific surface area is 4.3 $m^2.g^{-1}$. APP (AP423) was kindly supplied by Clariant. AP423 particles exhibit a 2 μm – 13μm average diameter and a 1.1 $m^2.g^{-1}$ specific surface area.

Sample preparation

All composite specimens were prepared by mixing PS powder, W fillers and APP additive. The global filler content was kept constant

* *Correspondence to: L. Ferry, Ecole des Mines d'Alès, Centre CMGD, 6 avenue de Clavières, F-30319 ALES CEDEX, France.*
E-mail: laurent.ferry@mines.ales.fr

Y.-T.-H. Quach, L. Ferry, R. Sonnier, J.-M. Lopez Cuesta
Ecole des Mines d'AlèsCentre CMGD6 avenue de Clavières, F-30319, ALES CEDEX, France

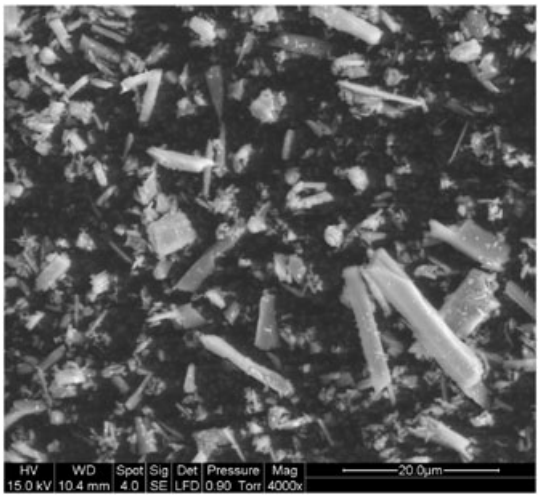

Figure 1. SEM image of wollastonite particles.

at 15 wt%. The proportions in which W and APP were combined are represented in the Table 1. Polymer and fillers were dried in vacuum at 80°C during 4 h before melt mixing. Blends of PS with fillers were compounded using an internal mixer (Haake Polylab) at 190°C and at 60 rpm for approximately 10 min. After mixing and cooling, the material was ground into pieces smaller than 10 mm in an Alpine grinder. Then, specimens ($100 \times 100 \times 4$ mm^3) were injection molded (50 Tons Krauss Maffei, 260°C) from the pellets, after air drying at 80°C for 4 h. All the samples used for testing were cut from these specimens.

Experimental techniques

Thermogravimetric analysis (TGA) was performed on a Perkin Elmer Pyris-1 TGA thermobalance operating under nitrogen in alumina crucibles containing around 10 ± 2 mg of material and ranging from 30°C to 900°C at a heating rate of 10°C.min^{-1}.

The cone calorimeter, manufactured by Fire Testing Technology (FTT), is a standard apparatus used for fire retardancy tests (ISO 5660). The polymer sample ($100 \times 100 \times 4$ mm^3) is placed horizontally on a balance and irradiated from above (50 kW/m^2). Tests were carried out with a piloted ignition in air. We will focus here on the heat release rate (HRR) curves determining the peak of HRR (peak HRR), total heat release (THR), times to ignition (TTI), effective heat of combustion (EHC). Results correspond to mean values obtained from two or three experiments. The HRR uncertainty is estimated to 10%.[30,31] Residues obtained after cone calorimeter tests were used for further characterization by energy dispersive X-ray spectroscopy (EDS), scanning electron microscopy (SEM) and X-ray diffraction (XRD).

Table 1. Composition of PS composites containing Wollastonite and APP additives

Nomenclature	Composition (wt%)		
	PS	Wollastonite	APP
PS	100	0	0
PS85APP15	85	0	15
PS85W3APP12	85	3	12
PS85W5APP10	85	5	10
PS85W7.5APP7.5	85	7.5	7.5
PS85W10APP5	85	10	5
PS85W12APP3	85	12	3
PS85W15	85	15	0

Pyrolysis-combustion flow calorimeter (PCFC) is an apparatus developed firstly by Lyon for Federal Aviation Administration. PCFC enables to study the flammability of samples as small as 1–3 mg. The HRR is calculated according to oxygen depletion, like in cone calorimeter test. The great interest of this test is the separation between the pyrolysis of the solid and the combustion of the gases released during the degradation. More details are given elsewhere.[32] PCFC (supplied by FTT, Great Britain) was used in standard conditions: the sample was heated up to 750°C at a rate of 1°C/s in pure nitrogen. The gases were evacuated to the oven and the combustion occurred at 900°C in a N_2/O_2 (80/20) atmosphere. The uncertainty is estimated to 5%.

The fire behavior was also characterized by infrared pyrometry coupled "epiradiator test" (French standard NFP 92–505). $70 \times 70 \times 4$ mm^3 specimens are exposed to a 500 W radiator. Samples are placed on a grid located 30 mm under the bottom of the epiradiator. The heat flux on the surface of the sample was measured equal to 37 kW/m^2. The infrared pyrometer (Optris CT) is placed in appropriate position above the epiradiator and is removed every 12 s during 1 s approximately in order to measure the surface temperature of the sample.

PyGC/MS analyses were performed with a Pyroprobe 5000 pyrolyser equipped with CDS Analytical for flash pyrolysis in a helium environment. The samples were heated at T_{TGA} (temperature at the maximal mass loss rate obtained by TGA). The temperature was held for 5 s then the gases were drawn to the gas chromatograph for 5 min. The pyroprobe 5000 is interfaced to a 450-GC gas chromatograph (Varian). In the oven, the initial temperature of 70°C was raised to 290°C at 20°C/min. The column is a Varian Vf-5ms capillary column (30 m $\times$ 25 mm) and helium (1 mL/min) was used as the carrier gas. The gases were introduced from the GC transfer line to the ion trap analyzer of the 240-MS mass spectrometer (Varian) through the direct-coupled capillary column. Initial sample weight was less than one mg for each experiment.

Images of composites were obtained with a SEM microscope (FEI Quanta 200 SEM) using secondary electron or backscattered electron detectors. All images were obtained under high vacuum at a voltage of 12.5–15 kV with a spot size of 3–4 and a working distance of 6–12 mm. Composites were observed after fracture in liquid nitrogen whereas residues were imaged without any preparation. Energy dispersive X-ray spectroscopy (EDX) performed with the same device was used to obtain information about sample surface composition.

XRD patterns were recorded on a Bruker AXS D8 Advance X-ray powder diffractometer using the Cu Kα radiation. The powders were compacted with a glass slide for analysis.

RESULTS AND DISCUSSION

Dispersion of the fillers

The dispersion of the fillers in the polymer is very important for the properties of the composites.[2–4,33] At low magnification, SEM shows that the W and APP are well dispersed throughout the polymer (Fig. 2a and 2b). However, there is a small difference

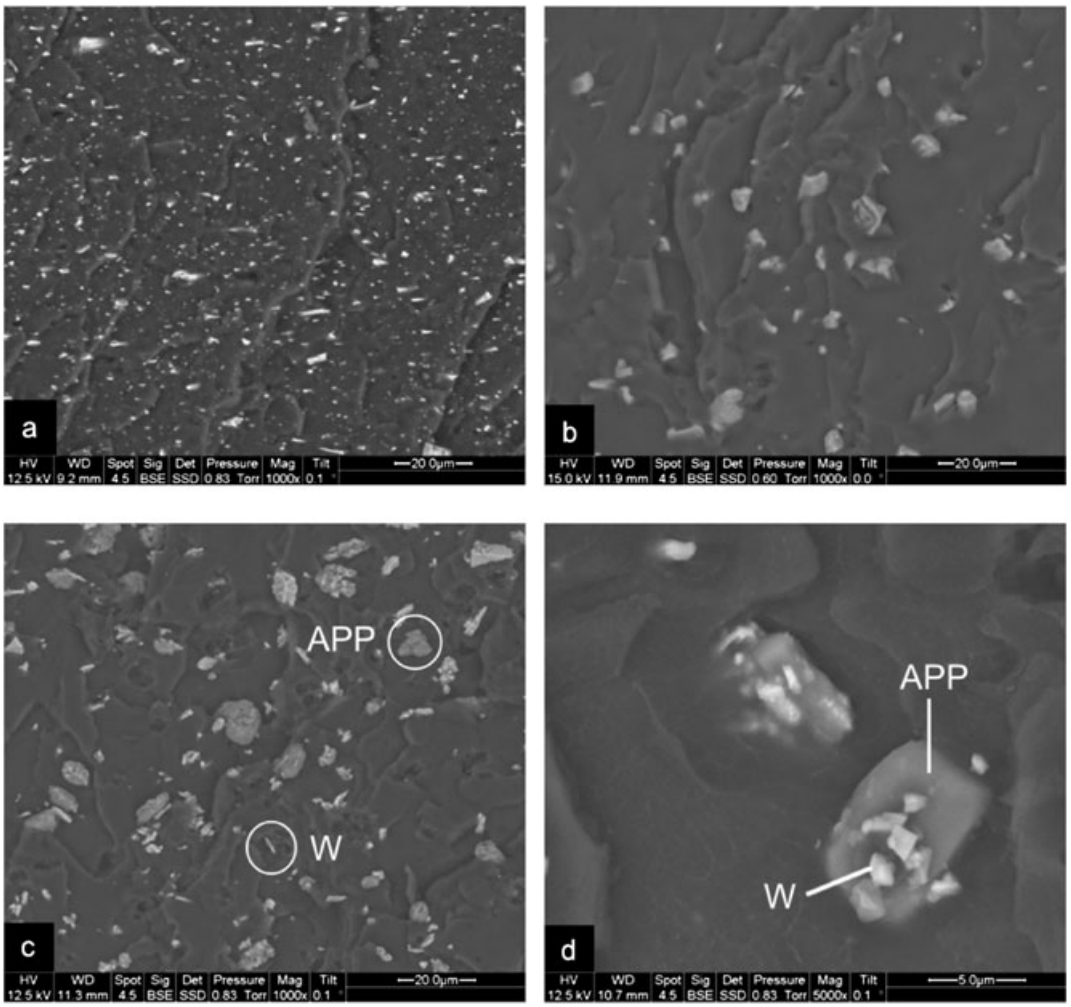

Figure 2. SEM photographs of (a) PS85W15, (b) PS85APP15 (c) PS85W7.5APP7.5 at low magnification, (d) PS85W7.5APP7.5 at high magnification. Photographs are representative of W/APP composites.

between the size of the fillers. W particles are thinner and less agglomerated than APP particles. In the PS/W/APP composites (Fig. 2c), the dispersion of APP fillers is similar to that of PS/APP composites. At high magnification (Fig. 2d), the presence of W particles on the surface or inside the agglomerated APP was observed. Thus, W and APP particles are in close contact. This proximity can favor the synergic effect between both fillers if it happens as it was shown in our previous study on PMMA composites containing APP and silica.[33]

Thermogravimetric analysis

Figure 3 shows the TGA and DTG curves of pure PS and PS composites between 350 and 500°C under N_2.

The mechanism of the thermal degradation of PS is considered to be a radical chain reaction. Styrene is produced in a free radical process which proceeds by elimination from the secondary macroradical of PS.[17] Decomposition of PS85APP15 follows the thermal behavior of unfilled PS until 400°C. Then, stabilization occurs and a char is formed. Czegeny *et al.* [17] explain that modifications of the degradation pathway of PS occur in the presence of APP and polyphosphoric acid. On one hand, backbiting of PS is not favored owing to a decrease of macroradical reactivity resulting from change of electron donating ability of the phenyl side group. On the other hand, interactions between ionic species of the phosphorus additive and radical sites lead to cyclization reactions and promote char formation. The addition of APP makes the maximal mass loss rate to be lower but its peak widens.

Theoretical residues of composites ($Comp_{res}^{th}$) have been calculated by two methods. The first one considers a linear mixing rule on the residues of the different components:

$$Comp_{res}^{th1} = x_{PS} \times PS_{res}^{exp} + x_{AP} \times APP_{res}^{exp} + x_W \times W_{res}^{exp} \quad (1)$$

Where x_{PS}, x_{AP} and x_W represent the weight fraction of PS, APP and W. PS_{res}, APP_{res} and W_{res} are the experimental residues at 700°C of pure PS, APP and W. The comparison of $Comp_{res}^{th1}$ with experimental residues enables to highlight the global interaction between components in the condensed phase.

The second method consists in calculating the theoretical residue of ternary composition using a mixing rule between binary compositions:

$$Comp_{res}^{t\,h2} = y_{APP} \times PS85APP15_{res}^{exp} + y_W \times PS85W15_{res}^{exp} \quad (2)$$

where y_{APP} and y_W represent the weight fraction of APP and W in the APP/W blend. $PS85APP15_{res}$ and $PS85W15_{res}$ are the experimental residues at 700°C of the corresponding composites.

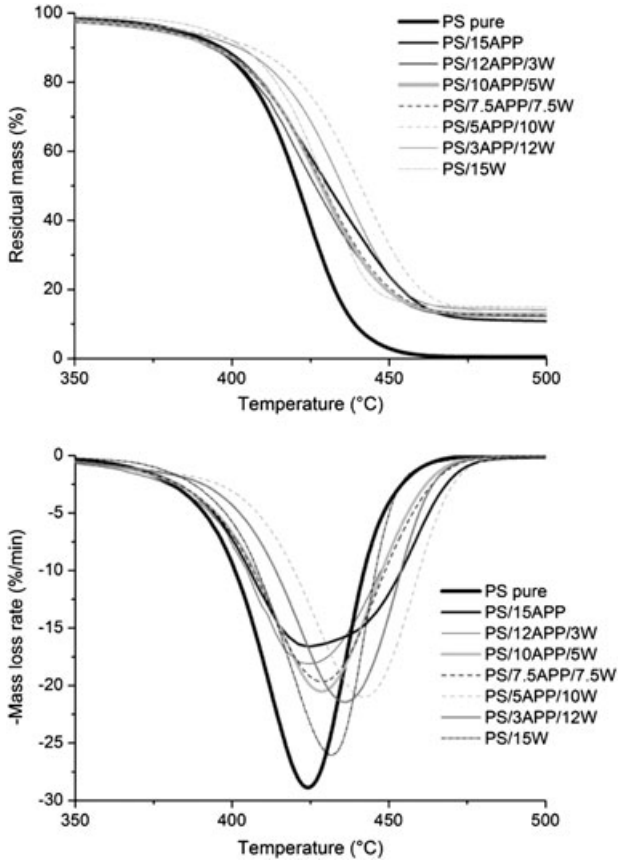

Figure 3. TGA and DTG curves of pure PS and various filled PS composites, under N2.

Since the calculation still considers the binary interactions, the comparison of $Comp_{res}^{th2}$ with experimental residues enables to highlight the additional effect due to specific interaction between APP and W.

The experimental residue obtained at 700°C for all composites is higher than the theoretical residue $Comp_{res}^{th1}$ except in the case of PS85W15. The residues are particularly high for APP12W3 and APP10W5 compositions, highlighting a strong interaction between the components. The gap between the experimental and theoretical residues $Comp_{res}^{th1}$ in the case of PS/AP composite (1.11%) is explained by the formation of char. In order to assess if the combination of W with APP leads to supplementary char, $Comp_{res}^{th2}$ can be compared with experimental residues.

The results indicate that a significant part of the residue in the PS/W/APP composites is related to interaction of W with APP. It is suggested that this additional residue is linked to the content of phosphorus (P) in the composites. In PS/APP composite, a part of P leaves the condensed phase to the gas phase during the test whereas in PS/W/APP, W and APP may interact keeping a greater amount of phosphorus in the condensed phase. This assumption will be discussed later on.

Replacement of additive APP by 3%W, 5%W, 7.5%W or 15%W improves the thermal stability of the composites but not in a significant manner. However, when 10% or 12% of APP are replaced by W, the temperature at maximal mass loss rate (T_{TGA}) increases significantly (about 15°C) as shown in Table 2. It means that there is a range around 10 and 12% where substitution of APP by W induces an optimal efficiency on the thermal stability of composites. This particular thermal behavior of PS composites may be due to a synergistic effect of the W/APP system.

Fire properties

PCFC test

Table 3 lists PCFC results: heat release capacity (HRC, which is the peak HRR divided by the heating rate), THR, EHC (which is calculated from PCFC and TGA results eqns 3 and 4) and temperature at the maximum HRR (T_{PCFC}). A good correlation between the T_{TGA} and the T_{PCFC} can be seen (see Fig. 4). The T_{PCFC} attain maximum values for both composites PS85W12APP3 and PS85W10APP5 as in the case of T_{TGA}. However, the temperature at maximum HRR is higher than in TGA. It is so understandable because the heating rate in PCFC (1°C.s^{-1}) is higher than the heating rate in TGA (10°C.min^{-1}).[34] Table 3 shows a reduction in the THR_{PCFC}, EHC_{PCFC} of the PS composites in comparison with pure PS. Beside the calculated EHC_{PCFC} value (eqn 3), another parameter noted EHC^*_{PCFC} (eqn 4) was used:

$$EHC_{PCFC} = \frac{THR_{PCFC}}{Mass\,Loss_{TGA}} \tag{3}$$

$$EHC^*_{PCFC} = \frac{THR_{PCFC}}{Mass\,Loss_{combustible\,gas}} = \frac{THR_{PCFC}}{Mass\,Loss_{TGA} - \%NH_3^{evap}} \tag{4}$$

where $\%NH_3^{evap}$ corresponds to the weight fraction of ammoniac released from APP in the gas phase.

The EHC^*_{PCFC} is attributed to EHC of combustible gases which are released from the PS polymer in PS composite. In other

Table 2. TGA results of PS composites. The difference between experimental and calculated residue was indicated in brackets

Composition (wt%)	T_{TGA} (°C)	Maximal mass loss rate (%/min)	Residue at 700°C (%)	$Comp_{res}^{th1}$ (%)	$Comp_{res}^{th2}$ (%)
PS	424	29.4	0.21	0.21	-
PS85APP15	428	16.7	8.41	7.30 (1.11)	8.41
PS85W3APP12	428	18.9	11.37	8.85 (2.52)	9.65 (1.72)
PS85W5APP10	430	20.3	12.24	9.88 (2.36)	10.45 (1.79)
PS85W7,5APP7,5	430	19.6	11.90	11.17 (0.73)	11.50 (0.4)
PS85W10APP5	440	21.0	13.71	12.45 (1.26)	12.55 (1.16)
PS85W12APP3	442	21.3	13.90	13.48 (0.42)	13.35 (0.55)
PS85W15	427	25.1	14.59	15.03 (−0.44)	14.59

Table 3. PCFC parameters for PS and PS composites

Composition (wt%)	T_{PCFC} (°C)	HRC (J/g.K)	THR_{PCFC} (kJ/g)	EHC_{PCFC} (kJ/g)	EHC^*_{PCFC} (kJ/g)
PS	434	894 (0%)	36.8	36.8	36.8
PS85APP15	435	481 (– 46%)	29.5	32.2	33.1
PS85W3APP12	436	567 (– 37%)	30.1	33.9	34.7
PS85W5APP10	440	568 (– 36%)	29.8	34.0	34.6
PS85W7.5APP7.5	436	550 (– 38%)	29.6	33.5	34.0
PS85W10APP5	446	592 (– 34%)	30.5	35.3	35.7
PS85W12APP3	443	565 (– 37%)	29.4	34.1	34.3
PS85W15	435	693 (– 22%)	28.8	33.7	33.7

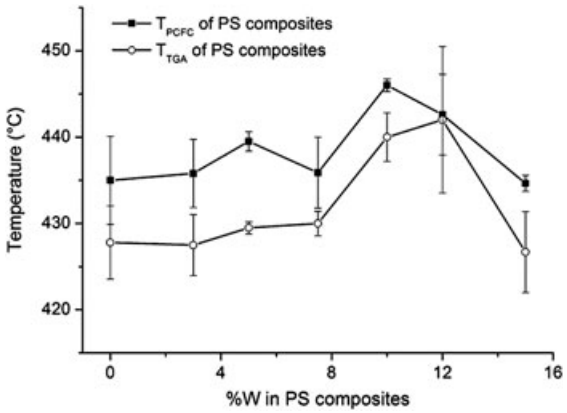

Figure 4. Comparison between the temperature at maximum heat release rate and the temperature at maximum mass loss rate in PCFC and TGA, respectively.

words, the release of NH_3 from the degradation of APP during the combustion is not taken into account in EHC^*_{PCFC}. It is noteworthy that the EHC^*_{PCFC} values of PS composites are lower than the EHC_{PCFC} values of pure PS. The combustion in the PCFC test is complete, so, this result shows that the combustible gases in the case of PS composites and in the case of pure PS are different. Similar to TGA results, it can be proposed that the presence of APP modifies the degradation pathway of PS,[17] thus the released combustible gases are different. Interestingly, W has the same influence as APP. The Py-GCMS analysis supplies data consistent with this observation. The compositions of the pyrolytic gases formed by pure PS and PS composites at about 450°C pyrolysis temperature are summarized in Table 4. In agreement with Czegeny,[17] some changes in the distribution of decomposition products are observed. The formation of toluene, ethylbenzene, alpha-methylstyrene are enhanced in presence of APP and W.

According to the PCFC test, HRC of the PS composites decreases in comparison with pure PS. A decrease of about 22% is observed in PS85W15. This value is only slightly higher than the percentage of W in the composite (15%). Therefore, the decrease may be mainly ascribed to a dilution effect (replacement of 15% pure PS by 15% W). Contrary to PS85W15, all other composites show a more significant reduction of HRC. The PCFC test needs a small amount, so at this scale, it is supposed that no barrier effect could be efficient. Therefore, APP and APP/W themselves can improve the fire behavior of PS composites at microscale level. In the following, the cone calorimeter test, which can give information about the fire behavior at macroscale level, will be performed.

Cone calorimeter

Cone calorimetry is a useful technique to evaluate fire behavior of polymers within the different stages of a developing fire.[35,36] The HRR curves as well as other cone calorimeter data of PS and PS composites are presented in Fig. 5 and Table 5. In the case of PS/APP composites, ignition arises 16 s before pristine PS owing to release of combustible compounds catalyzed by the presence of APP. That confirms modification of degradation pathway of PS induced by APP additives. HRR rapidly increases up to 500 kW/m^2 and then continues to increase more slowly up to about 900 kW/m^2 before falling down due to fuel depletion. The incorporation of APP solely (PS85APP15) is not efficient to decrease significantly the pHRR. It is in agreement with previous results which were performed under a 35kW/m^2 irradiance.[14] In the case of PS/W composites, the HRR curve exhibits a similar shape than that of PS/APP. However, PS85W15 shows a

Table 4. Relative area of Py/GC-MS peaks of the pyrolysis products from PS and PS composites (in the range 0 min $< t_R <$ 10 min, area peak of styrene is normalized to 100)

Composition (wt%)	Toluene	Ethylbenzene	Alpha-methylstyrene	Styrene
PS	0.90	0.12	0.15	100
PS85APP15	1.72	0.23	1.43	100
PS85W3APP12	1.80	0.46	0.87	100
PS85W5APP10	1.68	0.15	0.45	100
PS85W7.5APP7.5	2.33	0.23	0.55	100
PS85W10APP5	1.75	0.17	2.87	100
PS85W12APP3	2.58	0.78	0.58	100
PS85W15	1.61	0.51	0.46	100

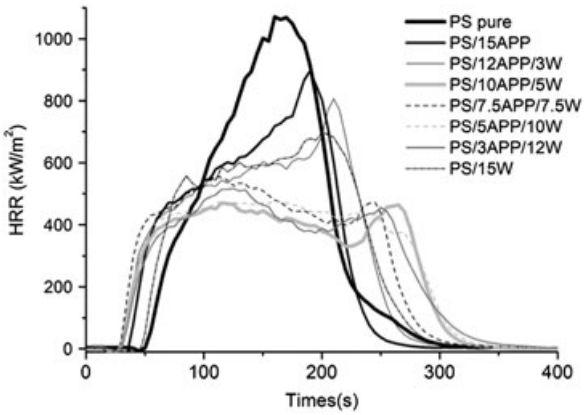

Figure 5. Heat release rate curves of PS and PS composites.

significant reduction of pHRR in comparison to pristine PS (−40%) and to PS85APP15 (−19%). Moreover, the time to ignition is somewhat similar to that of pure PS. Here, a specific action of W on the fire behavior is highlighted. In the case of ternary PS/W/APP composites, a reduction of time to ignition comparable to that of PS/APP is observed. The values of TTI seem not consistent with thermal stability as determined by TGA. However, this can be justified by the fact that time to ignition is a complex parameter that depends not only from the onset of degradation but also from other parameters such as thermophysical properties of materials (absorptivity, emissivity, thermal conductivity), migration of particles to the surface or convection in the melt. After ignition, ternary compositions enable to obtain better fire behavior with lower pHRR except for PS85W3APP12. In this latter composition, the ratio W/APP may be too low to generate a synergy. The HRR curves of PS/W/APP composites exhibit a shape different from those of PS/APP or PS/W: the peak HRR is reached more quickly at a lower level, and then the HRR exhibits a plateau which is typical of a barrier effect. At the end of the plateau, a small peak is observed. This peak, known as "heat feedback," is an experimental artefact which has already been assigned in the literature to the difference in thermal conductivity between the sample and the insulation backing. It can be noticed that heat feedback occurs all the later that the HRR plateau is low, highlighting the thermal shield effect of the formed surface layer. The pHRR are quite low showing a reduction of about 50–55% in comparison to pure PS. Similar to PCFC results, the THR and EHC of PS composites obtained by cone calorimetry are smaller than those of pristine PS. The combustion efficiency χ value (χ = EHC obtained by cone calorimeter/EHC obtained by PCFC) seems to be the same for all samples (~0,7). $\chi < 1$ is indicative of an incomplete combustion in the cone calorimeter. This latter remark indicates the formation of char residue that contributes to the beforementioned protective layer. To conclude, the combination of APP and W (more than 5%) improves noticeably the fire behavior of PS.

An insight on the sample residues after cone calorimeter test allows confirming definitely the results previously obtained. The residues of PS85W15, PS85W3APP12 and PS85APP15 are not cohesive. The residues are either very thin or there are large voids and cracks in the surface layer. On the contrary, for other composites, a more cohesive layer with a thicker and harder structure could be observed. The charred layer that develops in the early stages of combustion could protect the polymer surface by limiting the transfer of gas and heat (Fig. 6). The temperature of this charred layer during the combustion will be measured by "epiradiator test" (see below). Images of the surface residues obtained by SEM give us more information on this char layer. Figure 7 represents the SEM images of surface residues of PS/W/APP composites and PS85W15. At high magnification, it is observed that the higher the W content in the initial composites, the higher the number of W particles on the char layer. Also, the presence of APP in composites favors the appearance of char and this char contributes to bind the W particles to form a more cohesive layer. Moreover, it is possible that W particles react with APP particles during the combustion and form chemical bonding in the char. This assumption will be detailed with the characterization of the residues.

Epiradiator test

Under the epiradiator, at the moment of the ignition, the temperature of the sample surface increases quickly (about 400°C), and becomes quasi constant after a brief period. Figure 8 represents the temperature of the sample surface. It is an average of five measurements performed every 12 s after the ignition. It can be seen that the temperature of the surface layer of PS85W7.5APP7.5 and PS85W10APP5 is higher than that of the other compositions. The charred layer of PS/W/APP composite is thermally stable, and then its temperature could increase. According to the Stefan-Boltzmann law (eqn 5), the radiation of a material is proportional to the temperature at power 4. Therefore, the char dissipates more heat towards outside and less heat is absorbed by the non degraded polymer under char. Schartel has shown the influence of this effect in epoxy resins using

Table 5. Cone calorimetry data for PS and PS composites

Compositions	pHRR (kW.m^{-2})	TTI (s)	Residue at flame out (%)	THR (MJ.m^{-2})	EHC (kJ.g^{-1})	χ
Pure PS	1085 (0%)	41	0	126.2	27.4	0.75
PS85APP15	874 (−19%)	25	8.3	111.5	22.9	0.71
PS85W3APP12	805 (−26%)	21	11.5	115.1	26.9	0.79
PS85W5APP10	472 (−57%)	18	11.8	108.3	24.7	0.73
PS85W7.5APP7.5	556 (−49%)	18	12.2	111.1	25.6	0.76
PS85W10APP5	482 (−56%)	21	13.3	110.1	25.7	0.73
PS85W12APP3	512 (−53%)	21	13.4	105.7	25.1	0.74
PS85W15	653 (−40%)	39	14.2	109.7	26.2	0.78

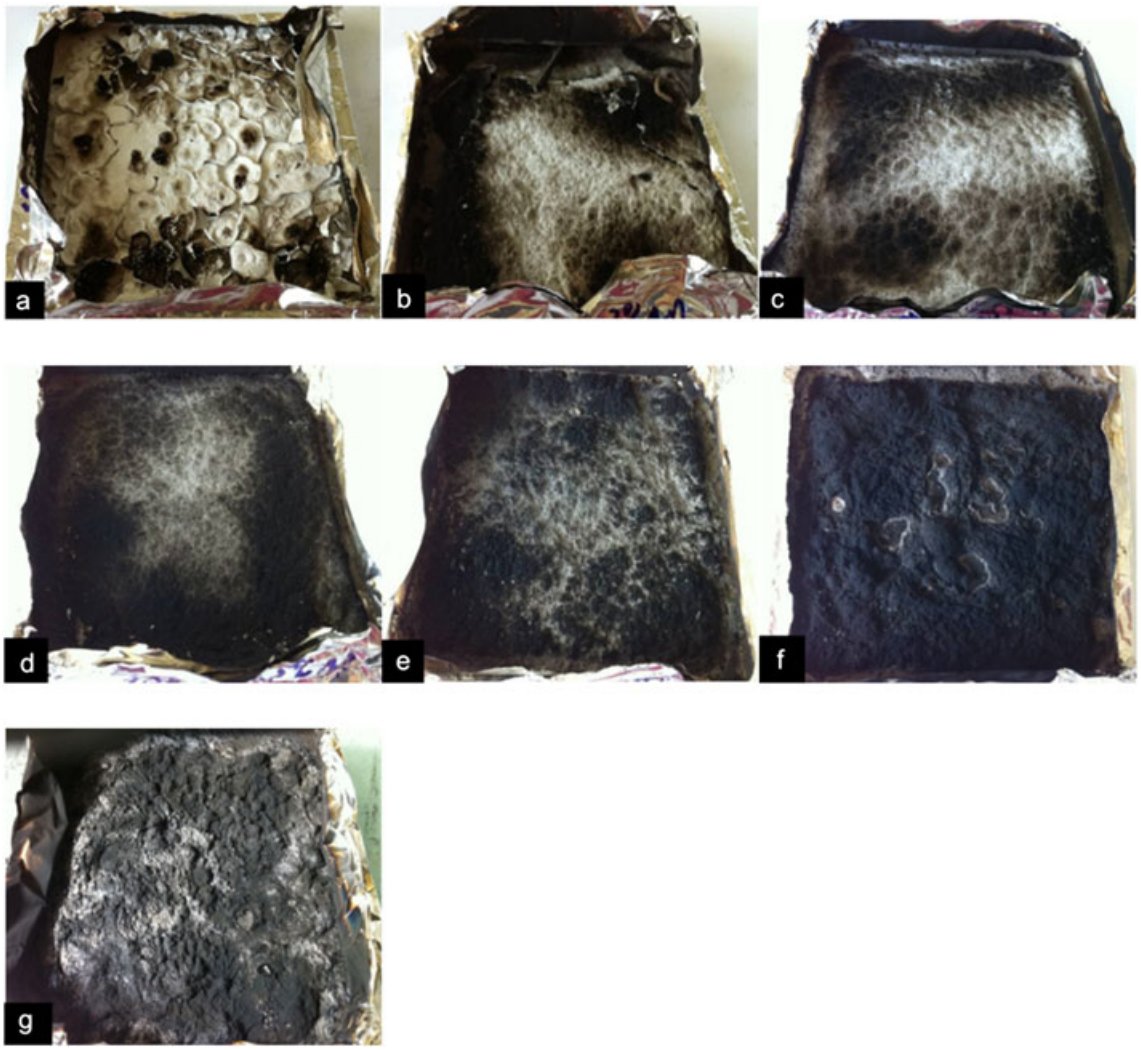

Figure 6. Photographs of char residues after cone calorimeter experiments on PS composites: a) PS85W15, b) PS85W12APP3, c) PS85W10APP5, d) PS85W7.5APP7.5, e) PS85W5APP10, f) PS85W3APP12, g) PS85APP15. This figure is available in colour online at wileyonlinelibrary.com/journal/pat

thermocouples.[37] A quick calculation allows estimating the heat dissipated by the different formulations, considering an emissivity of 1 (corresponding to a black body, not representative of our materials). For PS85W15 and PS85APP15 (surface temperature 460°C), the dissipated heat flux is close to 16 $kW.m^{-2}$. For PS85W3APP12, PS85W5APP10 and PS85W12APP3 (surface temperature 480°C), the dissipated heat flux is slightly higher: 18 $kW.m^{-2}$. In the case of PS85W7.5APP7.5 and PS85W10APP5 (surface temperature 520°C), the heat dissipation is 22 $kW.m^{-2}$. Therefore, these calculations indicate that the difference in re-radiation is always lower than 6 $kW.m^{-2}$. This difference is much reduced comparing to those calculated by Schartel and Weib [37]. It could be assumed that re-radiation by the charred layer is not the main mode-of-action of the flame-retardant additives in our materials.

$$J = \varepsilon \sigma T^4 \tag{5}$$

where J is the energy radiated by a real body (in $J.s^{-1}.m^{-2}$), ε its emissivity, T its temperature (in K) and σ the Stefan constant (5.67 10^{-8} $J.s^{-1}.m^{-2}.K^{-4}$)

Characterization of the residues

EDX analysis of residues

To quantify the presence of chemical elements in the residues, EDX analysis was performed during SEM observation. Two kinds of measurement for each composite were carried out: one is performed at the surface of the residue as collected after the fire test; the other was performed on the whole residue after grinding. Table 6 represents compositions of residues and of surface residues.

The comparison between Table 6a and b indicates that the main difference between surface composition and mean composition of residues affects carbon. The presence of carbon is more pronounced at the surface inducing a slight decrease in the content of the other elements. This result confirms the observation of the Fig. 7 where the appearance of a char was observed in the presence of W. Exempt from this rule, PS85APP15 exhibits lower carbon content at the surface. Moreover, this is in agreement with the epiradiator measurements. A more stable charred layer allows reducing the oxidation of carbon in CO and CO_2 and an increase in surface temperature. Contrary to carbon, the presence of

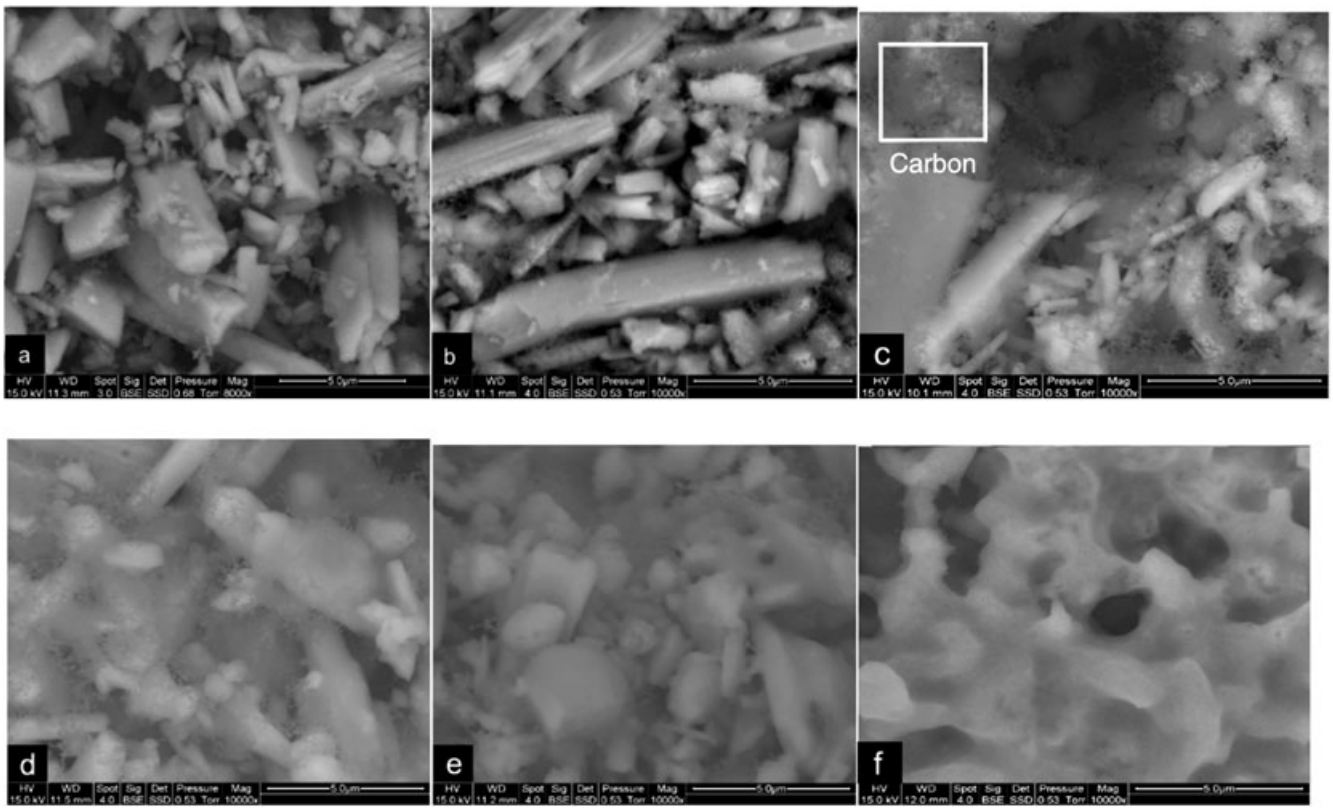

Figure 7. SEM images of residue surface of PS composites: a) PS85W15, b) PS85W12APP3, c) PS85W10APP5, d) PS85W7.5APP7.5, e) PS85W5APP10, f) PS85W3APP12.

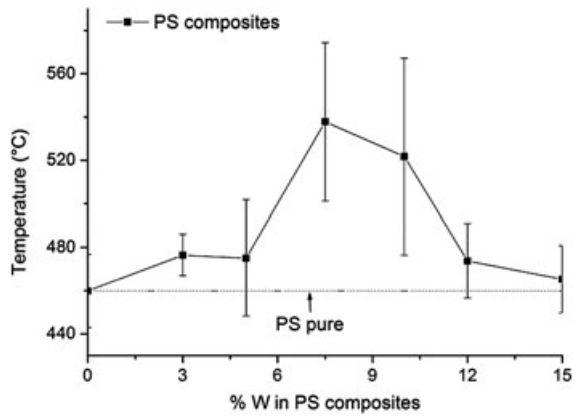

Figure 8. Temperatures of the surface of pure PS and PS composites under epiradiator during approximately 60 s after ignition.

phosphorus is lower at the surface than in the total residue. Calcium and silicon contents exhibit only small and not significant variations.

In order to understand whether the elements are released in the gas phase or if they remain in the condensed phase (residue), the percentages of P, Ca, Si after (X_1) and before (X_2) the combustion in cone calorimeter test (see Table 7) were calculated. $X_1 = X_2$ means that the element is remained in the condensed phase, $X_1 < X_2$ means that the element was partially released in the gas phase.

$$X_1 = \frac{\%P(\text{or Ca or Si})\text{in the residue}^* \times \%\text{residue at flame out}^*}{100} \quad (6)$$

$$X_2 = \frac{\%P(\text{or Ca or Si})\text{in APP(or W)} \times \%\text{APP(or W)in initial composite}}{100} \quad (7)$$

* see Table 6a

This calculation shows once again the stability of calcium and silicon percentage before and after the combustion indicating that W remains in the residue. The percentage of phosphorus before and after combustion changes weakly, except in the case of PS85APP15. This result supports the assumption that was made in paragraph 3.2 to interpret TGA results. In the case of PS85APP15, a significant part of phosphorus is released into the gas phase. This result is very consistent with values of EHC obtained by PCFC and cone calorimeter. The EHC of PS85APP15 is quite small (32.2 kJ/g with PCFC and 22.9 kJ/g with cone calorimeter) in comparison to the other composites (34–35 kJ/g with PCFC and 25–26 kJ with cone calorimeter).

In the PS/W/APP composites almost all phosphorus is held in the condensed phase during the combustion. This means that APP acts mainly in the condensed phase during the fire test. There are two hypotheses to explain the constancy of phosphorus amount before and after the combustion. Either phosphorus is held in the residue by the reaction between W and APP during the combustion or it is trapped by the char layer rich in W. To highlight these two hypotheses, XRD tests were performed.

Table 6. Quantitative analysis by SEM/EDX of: (a) residues and (b) surface of residues

a)

Compositions	%C	%O	%Si	%P	%Ca	%N	Residue at flame out (%)
PS85APP15	9.0	54.1	-	29.3	-	7.7	8.3
PS85W3APP12	5.0	49.0	6.0	31.5	8.5	Not detected	11.5
PS85W5APP10	4.6	46.9	9.1	29.3	14.1	Not detected	11.8
PS85W7.5APP7.5	4.2	44.2	13.7	16.9	21.0	Not detected	12.2
PS85W10APP5	2.3	41.7	19.5	8.8	27.7	Not detected	13.3
PS85W12APP3	1.9	40.9	21.7	4.7	30.8	Not detected	13.4
PS85W15	2.3	39.4	24.3	-	34.4	Not detected	14.2

b)

Compositions	%C	%O	%Si	%P	%Ca	%N
PS85APP15	2.0	51.4	-	33.0	-	13.7
PS85W3APP12	9.0	51.7	3.9	24.5	10.9	Not detected
PS85W5APP10	8.6	46.52	12.08	16.18	16.62	Not detected
PS85W7.5APP7.5	13.2	41.49	12.87	12.59	19.82	Not detected
PS85W10APP5	14.5	38.2	16.8	4.1	26.4	Not detected
PS85W12APP3	8.8	39.9	20	1.8	29.5	Not detected
PS85W15	3.6	37.6	22.8	-	36.0	Not detected

Table 7. Comparison of %P, %Ca, %Si in the composites before (X_1) and after (X_2) the combustion at cone calorimeter

Compositions	X_{1P}	X_{2P}	X_{1Ca}	X_{2Ca}	X_{1Si}	X_{2Si}
PS85APP15	2.7	4.8	0	0	0	0
PS85W3APP12	3.7	3.8	1.0	1.0	0.7	0.7
PS85W5APP10	3.0	3.2	1.7	1.7	1.1	1.2
PS85W7.5APP7.5	2.1	2.4	2.5	2.5	1.6	1.8
PS85W10APP5	1.2	1.6	3.8	3.4	2.7	2.4
PS85W12APP3	0.6	1.0	4.3	4.1	3.0	2.8
PS85W15	0	0	5.0	5.1	3.6	3.6

X-ray diffraction analysis

The XRD patterns (Fig. 9) of W/APP composites residues show the presence of W, calcium phosphate hydrate and silicon phosphate crystalline phases. The two latter crystals were identified through the presence of their main peaks ($2\theta = 7.6$ and 30.4 for calcium phosphate; $2\theta = 24.2$ and 27.3 for silicon phosphate). At high temperature, APP is decomposed and creates an acid medium which favors the reaction with W. Calcium phosphate and silicon phosphate are formed. In our previous work on PS/SiO_2/APP and PMMA/SiO_2/APP composite, SiP_2O_7 crystalline phase was also observed in the composite.[14,33] In the case of PS/Al_2O_3/APP, aluminum phosphate or metaphosphate were detected. To verify reaction between W and APP, XRD analyses were performed on mixtures of W + APP without PS (ratios in weight W/APP = 1/10, 3/10, 5/10) which were heated at 500°C during 5 min. Figure 10 represents the X-ray diffraction spectra of the residue of mixtures W + APP powder. The presence of SiP_2O_7 crystalline phase can clearly be observed at high APP content in the mixture. Moreover, ammonium calcium phosphate crystalline phase is also formed whatever the W/APP ratio. This type of phosphate is not observed in the

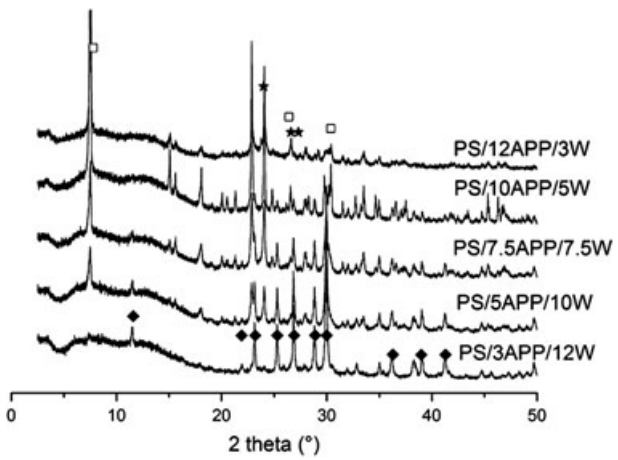

Figure 9. XRD patterns of residue of PS/APP/W composites. (♦) wollastonite CaSiO3, (⋆) silicon phosphate SiP2O7, (□) calcium phosphate hydrate Ca2P2O7 4H2O.

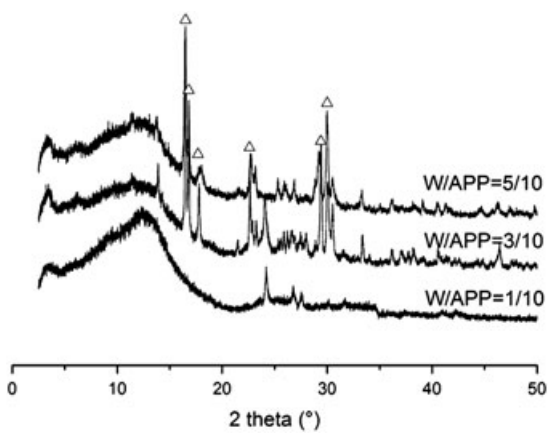

Figure 10. XRD patterns of mixtures of W+APP. (Δ) Ammonium calcium phosphate NH4CaP3O9.

residues of the PS/W/APP composite. Another type of calcium phosphate is formed, maybe due to different temperature and conditions in the cone calorimeter. Therefore, XRD enables to confirm the reaction between W and APP at high temperature. Based on the reaction between W and APP, and the results of Table 6, it can be concluded that the effect of APP in PS/W/APP composites occurs in the condensed phase. Finally, the fire behavior of PS/W/APP composites is improved thanks to synergy between these two fillers. These results are, to some extent, contradictory with those obtained previously by Duquesne *et al*.[38] or Isitman *et al*.[39] In these papers, the authors observed that the reactivity of APP with mineral fillers (talc or calcium carbonate) leads to the formation of magnesium or calcium phosphate that affects the expansion of the intumescent layer thus reducing the flame-retardant efficiency. However, it should be underlined that the above-mentioned papers refer to intumescent flame-retardant systems. In the present work, Fig. 6 reveals that PS/APP is not an intumescent system. Since the expansion of the residue is not the main fire retardant mechanism, the reactivity between W and APP may play a positive role on HRR reduction by increasing the cohesion of the protective layer as it was already observed with silica and alumina.[14]

CONCLUSION

The incorporation of W in combination with a phosphorous additive (APP) has given noteworthy flame-retardant properties to PS. Both fillers are well dispersed and contacted throughout the polymers. An improvement of the thermal stability as well as a reduction of the peak HRR was observed. In a particular range of W/APP ratio, a synergistic effect was even evidenced. The presence of 5%W in the W/APP composite seems enough to enhance the flame-retardant properties of PS. During the combustion, APP is decomposed to form an acid medium and promote the char formation. Acid medium favors the reaction between W and phosphorus compound. The constancy of P content in the sample before and after combustion indicates that the flame-retardant effect of APP is in the condensed phase. A cohesive residue layer is formed during the combustion. This layer consists mainly of W, carbon and a mixture of calcium and silicon phosphate which is thermally stable. The char contributes to link the W particles and to increase the cohesiveness of the surface layer. This residue layer limits the release of the combustible gas to the gas phase during the combustion. Finally, the combination of both fillers W and APP with an appropriate ratio can reinforce the flame retardancy of PS, as proved by the strong decrease of HRR.

Acknowledgements

We thank to CARNOT MINES Institute for supporting this work and to Nyco minerals, Clariant, Totalpetrochemicals for their products.

REFERENCES

[1] Gy. Marosi, A. Marton, A. Szep, I. Csontos, S. Keszei, E. Zimonyi, A. Toth, X. Almeras, M. Le Bras, *Polym. Degrad. Stab.* **2003**, *82*, 379.
[2] J. W. Gilman, C. L. Jackson, A. B. Morgan, Jr. R. Harris, *Chem. Mater.* **2000**, *12*, 1866.
[3] A. B. Morgan, Jr. R. Harris, T. Kashiwagi, L. J. Chyall, J. W. Gilman, *Fire mater.* **2002**, *26*, 247.
[4] J. W. Gilman, *Appl. Clay Sci.* **1999**, *15*, 31.
[5] J. Zhu, P. Start, K. A. Mauritz, C. A. Wilkie, *Polym. Degrad. Stab.* **2002**, *77*, 253.
[6] S. Hamdani, C. Longuet, D. Perrin, J. M. Lopez-Cuesta, F. Ganachaud, *Polym. Degrad. Stab.* **2009**, *94*, 465.
[7] J. Zhang, M. A. Delichatsios, S. Bourbigot, *Combust. Flame.* **2009**, *156*, 2056.
[8] B. Schartel, A. Weiß, H. Sturm, M. Kleemeier, A. Hartwig, C. Vogt, R. X. Fischer, *Polymers adv. technol.* **2011**, *22*, 1581.
[9] T. Kashiwagi, Jr. R. Harris, X. Zhang, R. M. Briber, B. H. Cipriano, S. R. Raghavan, W. H. Awad, J. R. Shields, *Polymer* **2004**, *45*, 881.
[10] B. N. Jang, M. Costache, C. A. Wilkie, *Polymer* **2005**, *46*, 10678.
[11] M. Lewin, *Polymers adv. technol.* **2006**, *17*, 758.
[12] B. Schartel, M. Bartholmai, U. Knoll, *Polym. Degrad. Stab.* **2005**, *88*, 540.
[13] M. Zanetti, S. Lomakin, G. Camino, *Macromol. Mater.Eng.* **2000**, *279*, 1.
[14] N. Cinausero, N. Azema, J. M. Lopez-Cuesta, M. Cochez, M. Ferriol, *Polym. Degrad. Stab.* **2011**, *96*, 1445.
[15] S. Chang, T. Xie, G. Yang, *Polym. Degrad. Stab.* **2006**, *91*, 3266.
[16] P. Kiliaris, C. D. Papaspyrides, *Prog. Polym. Sci.* **2010**, *35*, 902.
[17] Z. Czégény, M. Blazso, *J. Anal. Appl. Pyrolysis* **2008**, *81*, 218.
[18] N. Cinausero, N. Azema, J. M. Lopez Cuesta, M. Cochez, M. Ferriol, *Polymers adv. technol.* **2011**, *22*, 1931.
[19] N. Cinausero, Thermal degradation and fire reaction of PS and PMMA nanocomposites. Ph.D.Thesis, Université Montpellier 2, **2009**.
[20] N. Cinausero, N. Azema, M. Cochez, M. Ferriol, M. Essahli, F. Ganachaud, J. M. Lopez-Cuesta, *Polymers adv. technol.* **2008**, *19*, 701.
[21] K. H. Rao, K. S. E. Forssberg, W. Forsling, *Colloids Surf. A Physicochem. Eng. Asp.* **1998**, *133*, 107.
[22] R. S. Hadal, A. Dasari, J. Rohrmann, R. D. K. Misra, *Mater. Sci. Eng. A* **2004**, *372*, 296.
[23] S. Hamdani-Devarennes, A. Pommier, C. Longuet, J. M. Lopez-Cuesta, F. Ganachaud, *Polym. Degrad. Stab.* **2011**, *96*, 1562.
[24] U. A. Handge, K. Hedicke-Höchstötter, V. Altstädt, *Polymer* **2010**, *51*, 2690.
[25] A. S. Luyt, M. D. Dramicanin, Z. Antic, V. Djokovic, *Polymer Testing.* **2009**, *28*, 348.
[26] K. L. Shephard, Flame resistant silicone rubber wire and cable coating composition. US Patent 6,239,378. **2001**.
[27] C. George, A. Pouchelon, R. Thiria, Composition polyorganosiloxanes vulcanisables à chaud utilisable notamment pour la fabrication de fils ou câbles électriques. French Patent 2,899,905. **2006**.
[28] Y. Zhang, Y. Liu, Q. Wang, *J. Appl. Polym. Sci.* **2010**, *116*, 45.
[29] Y. L. J. Liu, Q. Wang, *J. Appl. Polym. Sci.* **2009**, *113*, 2046.
[30] J. W. Gilman, T. Kashiwagi, M. Nyden, J. E. T. Brown, C. L. Jackson, S. Lomakin, In: *Chemistry and technology of polymer additives* (Eds: S. Al-Maliaka, C. A. Wilkie), Blackwell Scientific, London, **1999**, p 249–265.
[31] L. Clerc, L. Ferry, E. Leroy, J. M. Lopez-Cuesta, *Polym. Degrad. Stab.* **2005**, *88*, 504.
[32] R. E. Lyon, R. N. Walters, *J. Anal. Appl. Pyrolysis* **2004**, *71*, 27.
[33] Y. Quach, N. Cinausero, R. Sonnier, C. Longuet, J. M. Lopez-Cuesta, *Fire. mater.*, **2011**; accepted: DOI: 10.1002/fam.1119
[34] B. Schartel, K. H. Pawlowski, R. E. Lyon, *Thermochimica Acta.* **2007**, *462*, 1.
[35] S. Kim, C. A. Wilkie, *Polymer adv. technol.* **2008**, *19*, 496.
[36] B. Schartel, T. R. Hull, *Fire Mater.* **2007**, *31*, 327.
[37] B. Schartel, A. Weiß, *Fire mater.*, **2010**, *34*, 217.
[38] S. Duquesne, F. Samyn, S. Bourbigot, P. Amigouet, F. Jouffret, K. Shen, *Polymers adv. technol.*, **2008**, *19*, 620
[39] N. A. Isitman, M. Dogan, E. Bayramli, C. Kaynak, *Polymer eng. sci.* **2011**, *51*, 875.